

## Tomographic readout of an opto-mechanical interferometer

This content has been downloaded from IOPscience. Please scroll down to see the full text.

2012 New J. Phys. 14 095018

(<http://iopscience.iop.org/1367-2630/14/9/095018>)

View [the table of contents for this issue](#), or go to the [journal homepage](#) for more

### Download details:

IP Address: 194.95.157.141

This content was downloaded on 03/08/2016 at 09:01

Please note that [terms and conditions apply](#).

## Tomographic readout of an opto-mechanical interferometer

Henning Kaufer, Andreas Sawadsky, Tobias Westphal,  
Daniel Friedrich<sup>1</sup> and Roman Schnabel<sup>2</sup>

Institut für Gravitationsphysik, Leibniz Universität Hannover and Max-Planck  
Institut für Gravitationsphysik (Albert-Einstein-Institut), 30167 Hannover,  
Germany

E-mail: [roman.schnabel@aei.mpg.de](mailto:roman.schnabel@aei.mpg.de)

*New Journal of Physics* **14** (2012) 095018 (7pp)

Received 27 April 2012

Published 21 September 2012

Online at <http://www.njp.org/>

doi:10.1088/1367-2630/14/9/095018

**Abstract.** The quantum state of light changes its nature when being reflected off a mechanical oscillator due to the latter's susceptibility to radiation pressure. As a result, a coherent state can transform into a squeezed state and can get entangled with the motion of the oscillator. Full information of the state of light can only be gathered by a tomographic measurement. Here we demonstrate a tomographic interferometer readout by measuring arbitrary quadratures of the light field exiting a Michelson–Sagnac interferometer that contains a thermally excited high-quality silicon nitride membrane. A readout noise of  $1.9 \times 10^{-16} \text{ m Hz}^{-1/2}$  around the membrane's fundamental oscillation mode at 133 kHz has been achieved, going below the peak value of the standard quantum limit by a factor of 8.2 (9 dB). The readout noise was entirely dominated by shot noise in a rather broad frequency range around the mechanical resonance.

<sup>1</sup> Present address: Institute for Cosmic Ray Research, The University of Tokyo, 5-1-5 Kashiwa-no-Ha, Kashiwa, Chiba 277-8582, Japan.

<sup>2</sup> Author to whom any correspondence should be addressed.



Content from this work may be used under the terms of the [Creative Commons Attribution-NonCommercial-ShareAlike 3.0 licence](https://creativecommons.org/licenses/by-nc-sa/3.0/). Any further distribution of this work must maintain attribution to the author(s) and the title of the work, journal citation and DOI.

Experiments in quantum opto-mechanics seek to create and study pure quantum states in compound systems of mechanical oscillators and light. Recently, the quantum mechanical ground state of a mechanical oscillator was reached using laser cooling based on the light's radiation pressure [1]. Radiation pressure coupling of light and mechanical devices also forms the basis of proposals to produce (ponderomotively) squeezed and entangled states of light [2, 3] as well as to produce entanglement between light fields and mechanical motion [4, 5] or between two mechanical objects [6–8] providing a means of reliable storage of quantum states [9]. Tomographic characterizations [10, 11] of the optical and mechanical subsystems involved are necessary to provide a full description of the quantum state including, for instance, the squeezing parameter and the squeezing angle. For an optical field, the tomographic characterization can be done by subsequent ensemble measurements of (non-commuting) field quadratures using a balanced homodyne detector (BHD) [12]. Whereas a BHD is a standard tool in quantum optics, it has so far only rarely been used in opto-mechanical experiments. Recently, BHDs were used to measure the phase quadrature amplitude of a light field from an opto-mechanical cavity [13, 14]. A tomographic characterization of the output field was not performed.

Here we apply a tomographic characterization to the optical subsystem of an opto-mechanical Michelson–Sagnac interferometer. The interferometer contained a silicon nitride membrane as a translucent, high-quality mechanical oscillator. The tomographic characterization was performed over a broad frequency band around the oscillator's fundamental resonance frequency at about 133 kHz using a BHD whose local oscillator (LO) phase could be set to arbitrary values. We show that for quadrature angles close to the phase quadrature, the noise spectra were shot noise limited even at frequencies close to the thermally excited membrane resonance.

In figure 1, the Michelson–Sagnac interferometer of our experiment is sketched within the dashed circle. It consisted of a balanced (50/50) beam splitter and two steering mirrors forming its Sagnac mode. A commercially available silicon nitride (SiN) membrane [15] was placed in the center of the folded arms. The reflected parts of the light overlapped with the respective transmitted parts and formed the interferometer's Michelson mode, which was sensitive to a displacement of the membrane. The interference of all four beams at the beam splitter toward the interferometer's signal output was controlled to be destructive in order to provide a so-called 'dark port'. A detailed description can be found in [16]. The topology's quantum noise contributions have been theoretically analyzed in [17] and the first experimental realization of the topology was reported in [16, 18] using a conventional single photodiode readout. Recently, the Michelson–Sagnac topology was theoretically investigated in view of the realization of dissipative opto-mechanical coupling [19].

The membrane used in this work had a measured power reflectivity of  $R = 17\%$  at a laser wavelength of 1064 nm under normal incidence. We also determined the membrane's Brewster angle and deduced the index of refraction to  $n_{\text{SiN}} = 2.2$  in agreement with the value given in [20] for the same type of membrane. From the reflectivity and the index of refraction value, we deduced the membrane thickness to be 40 nm. This together with the membrane's side length of 1.5 mm results in an effective mass of  $m = 80$  ng [18]. The interferometer was operated inside a vacuum chamber to avoid gas damping or excitation of the membrane motion. We determined the mechanical quality factor  $Q$  of the fundamental oscillation mode for different pressures. As a result, we found  $Q = 6 \times 10^5$  for gas pressures below  $4 \times 10^{-6}$  mbar.

A piezoelectric element (piezo) actuated the membrane's position such that the carrier light destructively interfered in the interferometer's signal output port. The input light was thus

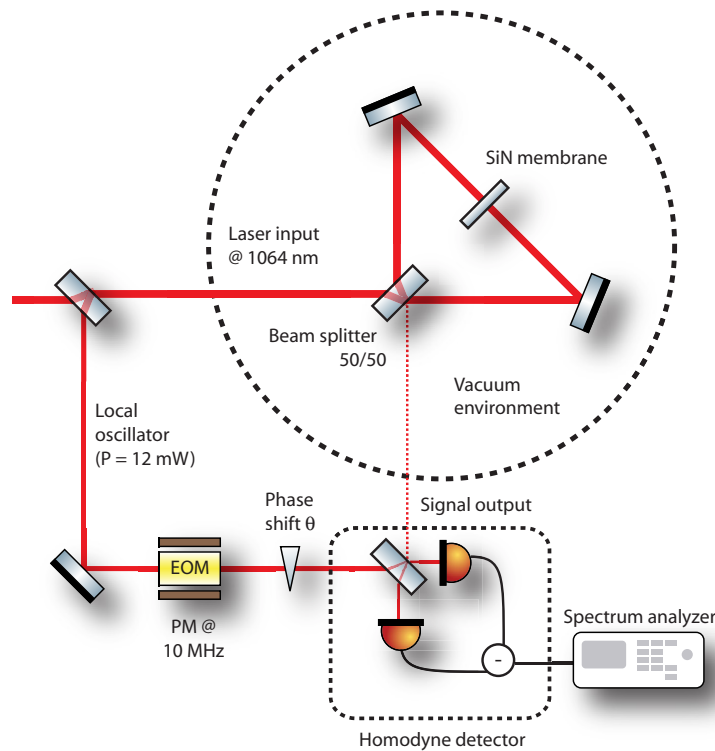


**Figure 1.** Simplified sketch of the Michelson–Sagnac interferometer with homodyne readout scheme. The laser light is split by a balanced beam splitter and recombined after reflection at the membrane. Signal sidebands leak out the dark port and are overlapped with a strong LO on a second (homodyne) beam splitter. An electro-optical modulator (EOM) provided a phase modulation to generate an error signal for locking the homodyne readout phase  $\theta$ .

back-reflected toward the laser source. The signal field mainly contained the upper and lower sideband fields that were produced by the thermally excited membrane motion. To accomplish the tomographic readout, the output field was overlapped with an external LO field of the same optical frequency as the interferometer's input on a 50/50 beam splitter. The light of the two beam splitter output ports was directed to two photodiodes forming a BHD. The difference of the photocurrents depends on the relative phase  $\theta$  between the LO and signal field and can be written as

$$i_-(\theta) \propto \alpha_{\text{LO}} X_\theta = \alpha_{\text{LO}} (\cos(\theta) X_1 + \sin(\theta) X_2). \quad (1)$$

Here,  $\alpha_{\text{LO}}$  is the coherent amplitude of the local oscillator,  $X_1$  and  $X_2$  are the amplitude and phase quadrature amplitudes of the signal field with respect to its coherent amplitude and  $X_\theta$  is the quadrature amplitude at a phase angle  $\theta$ . Note that the above equation is only valid if  $\alpha_{\text{LO}}$  is much bigger than the coherent amplitude of the signal beam, which is close to zero (exactly zero in the case of perfect interferometer contrast) for the interferometer operated on its dark port.

The membrane's thermally driven motion generates an excitation of the reflected light's phase quadrature, which is converted to an amplitude quadrature excitation of the interferometer's output field by the interference at the beam splitter. Conversely, the output

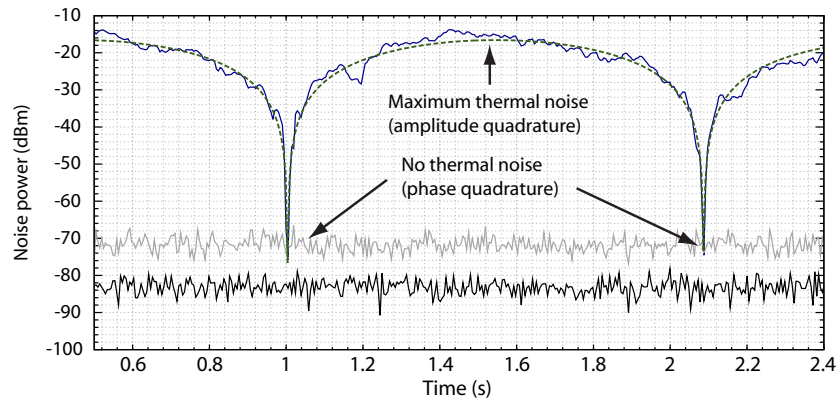


**Figure 2.** Zero-span noise-power measurement at the membrane's fundamental resonance frequency  $f_{\text{res}} = 133.88$  kHz. The readout phase  $\theta$  is scanned continuously. The blue curve shows the measured noise power, the dashed green line its theoretical model, and the gray curve shows the independently measured shot noise. For a particular quadrature phase ( $\theta = \pi/2$ ), no membrane displacement but only shot noise was measured. The black curve shows electronic dark noise. The resolution bandwidth (RBW) was set to 10 kHz.

field's phase quadrature is a measure of the differential amplitude quadrature excitation in the two arms of the interferometer. Due to the strong laser noise rejection at the Michelson dark port this excitation is given by optical quantum noise, i.e. by shot noise.

Figure 2 shows a zero-span measurement of the noise power at the membrane's resonance frequency  $f_{\text{res}}$  while the readout quadrature angle  $\theta$  was scanned by a piezo-driven mirror. This measurement is a tomographic readout because it allows for reconstruction of the output light's Wigner function. Indeed, the motion of the membrane is not visible in one particular quadrature angle where the noise power reaches shot noise. Note that squeezing is not expected in our setup owing to the low laser power and the high level of thermal noise.

In figure 3, measured spectra of the output light around the membrane's eigenfrequency are shown for various quadrature angles. For a readout quadrature of  $\theta = \pi/2$  almost no signal from the membrane excitation is visible. In figure 4, we present the broadband power spectrum for a frequency range from 10 kHz to 25 MHz. Here, we stabilized the readout homodyne phase to the amplitude quadrature  $\theta = 0$ . For this purpose, an EOM imprinted a phase modulation of  $f_{\text{mod}} = 10$  MHz on the LO beam. The homodyne signal was demodulated with the modulation frequency, generating an error signal for locking the homodyne readout phase via the above-mentioned piezo-driven mirror. The readout is limited by quantum shot noise for frequencies above 50 kHz.

In figure 5, we characterized the sensitivity of the Michelson–Sagnac interferometer with BHD readout for three different interferometer light powers. The spectra were converted into displacement spectral densities by the method described in [18] and independently by a calibrated piezo-driven membrane motion with  $f = 128$  kHz. Starting from  $P_{\text{in}} = 20$  mW we increased the input power to 200 mW. The input power was measured directly in front of the beam splitter. The phase of the BHD's LO was controlled to the amplitude quadrature ( $\theta = 0$ ) and its power was  $P_{\text{LO}} = 12$  mW for all measurements. The signal power in all measurements was always less than 0.5 mW.

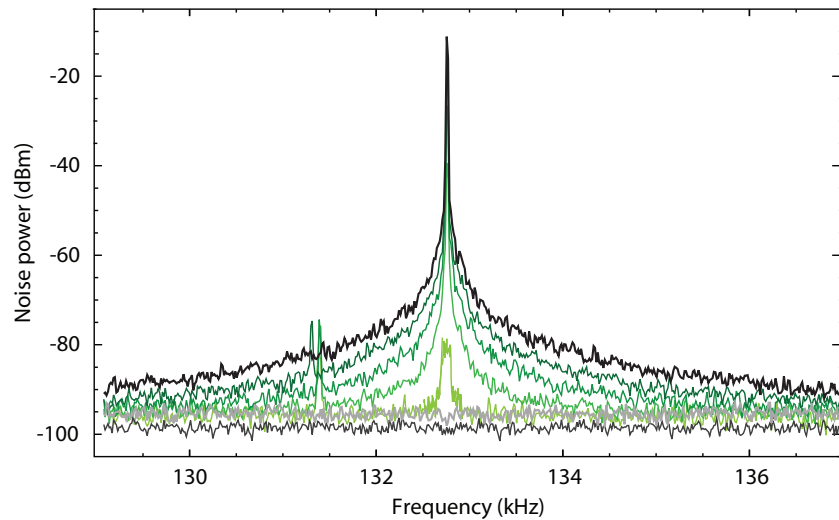


**Figure 3.** Noise power spectra taken for different values of the quadrature angle  $\theta$ . The top curve was taken with  $\theta = 0$  (black line) while the horizontal trace corresponds to shot noise (gray line). As  $\theta$  approaches  $\pi/2$ , less information about the membrane displacement is captured. Electronic dark noise is plotted in dark gray.

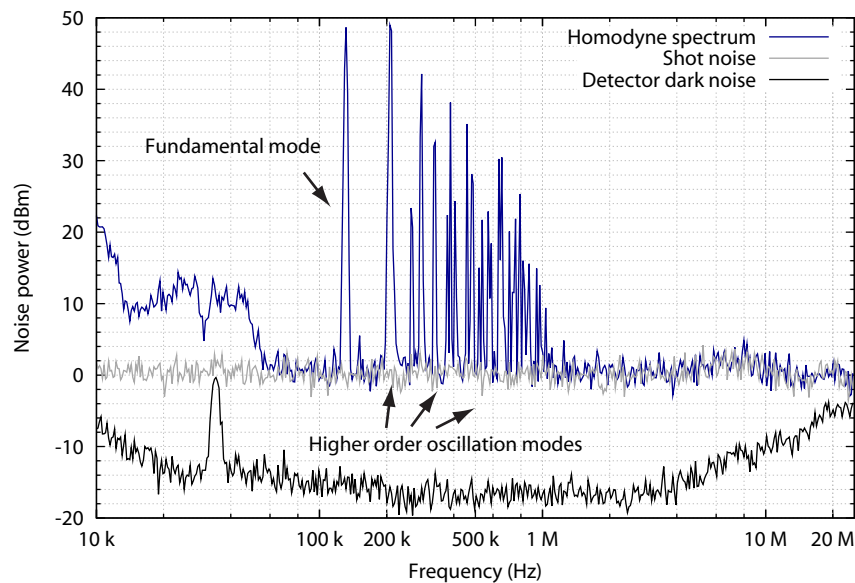


**Figure 4.** Noise power spectrum taken while  $\theta = 0$ . Above 50 kHz the spectrum is limited by optical shot noise. For smaller frequencies, acoustics and other noise sources are present. The upper readout limit of 25 MHz is set by electronics only. The RBW was 10 kHz and the data have been normalized by the modeled electronic transfer function of the photo detector. The bump at 8 MHz is due to imperfect modeling.

The quantum shot noise was measured by blocking the interferometer output at the BHD. A comparison between the calibrated shot noise and its theoretical prediction (1) carried out in [18] indicated an overall loss of 50% in the experiment. This value agreed with our

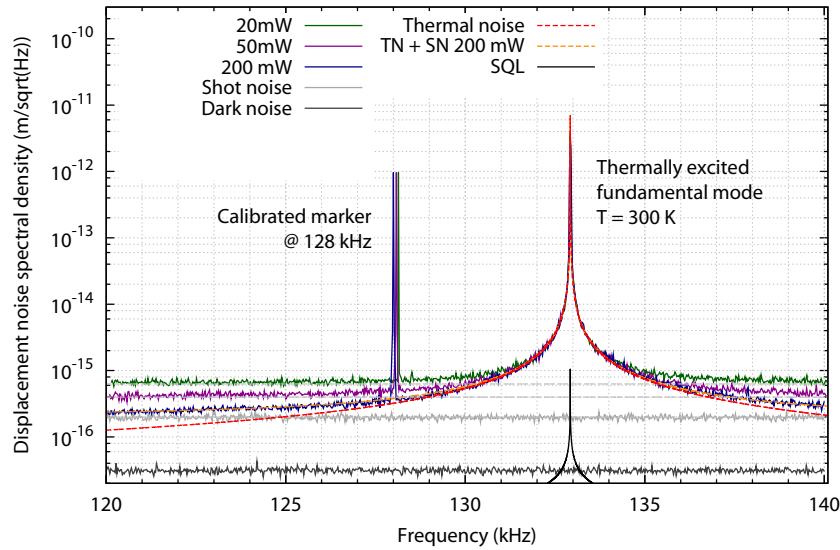


**Figure 5.** Calibrated spectra for different input powers  $P_{\text{in}}$ . The measured shot noise level for  $P_{\text{in}} = 200$  mW is plotted in gray. The corresponding electronic dark noise level is plotted as a brown line. Each dashed gray line indicates the calculated shot noise level for each individual input power. The orange dashed line shows the uncorrelated sum of shot noise and thermal noise for 200 mW input power. It is in excellent agreement with the measurement. The standard quantum limit is plotted as a solid black line. A defined displacement marker at 128 kHz is used for the calibration of the y-axis.

expectations and was given by the imperfect quantum efficiency of our BHD of separately measured 70% and imperfect reflectivities of the interferometer input and output optics. We expect that with better photo diodes and high-quality optics, the overall loss can be reduced to below 10% in future experiments. For each input power, the optical shot noise is plotted in gray (dashed lines). Off resonance, it is the dominant noise source within a broad frequency range from 50 kHz to 25 MHz in all measurements. For  $P_{\text{in}} = 200$  mW a displacement sensitivity of  $1.9 \times 10^{-16} \text{ m Hz}^{-1/2}$  at 120 kHz could be achieved. The orange dashed line corresponds to the uncorrelated sum of the thermal and shot noise. The gap between the three different measured shot noise levels exactly matches  $\sqrt{10}$  and  $\sqrt{4}$  as predicted by theory.

To conclude, we applied a tomographic readout to fully characterize the state of light being reflected off a thermally excited SiN membrane at room temperature. The readout was shot noise limited over a broad spectral region around the mechanical resonance and achieved an imprecision significantly below the standard quantum limit at the membrane's resonance frequency. In comparison to a simple amplitude quadrature readout using a single photodiode, the BHD has the advantage that the interferometer can be operated precisely at a dark port providing full laser noise rejection. Additionally, the readout LO acts as a mode-selective element, which is useful in discriminating residual transversal modes at the interferometer signal output port. Our setup is, in principle, able to detect non-classical properties of the output light such as ponderomotive squeezing [2] or could be part of an opto-mechanical entanglement analysis [4]. As the displacement sensitivity is limited by quantum shot noise, it could be enhanced by injecting squeezed states of light as demonstrated in numerous experiments [21–25].

## Acknowledgments

We acknowledge fruitful discussions with Y Chen, S L Danilishin, K Danzmann, K Hammerer, F Ya Khalili and H Miao. This work was supported by the International Max Planck Research School for Gravitational Wave Astronomy (IMPRS), and by the Centre for Quantum Engineering and Space-Time Research (QUEST). HK acknowledges support from the HALOSTAR scholarship program.

## References

- [1] Chan J, Alegre T P M, Safavi-Naeini A H, Hill J T, Krause A, Gröblacher S, Aspelmeyer M and Painter O 2011 *Nature* **478** 89–92
- [2] Mancini S and Tombesi P 1994 *Phys. Rev. A* **49** 4055–65
- [3] Wipf C, Corbitt T, Chen Y and Mavalvala N 2008 *New J. Phys.* **10** 095017
- [4] Vitali D, Gigan S, Ferreira A, Böhm H R, Tombesi P, Guerreiro A, Vedral V, Zeilinger A and Aspelmeyer M 2007 *Phys. Rev. Lett.* **98** 030405
- [5] Hunger D, Camerer S, Hänsch T W, König D, Kotthaus J P, Reichel J and Treutlein P 2010 *Phys. Rev. Lett.* **104** 143002
- [6] Müller-Ebhardt H, Rehbein H, Schnabel R, Danzmann K and Chen Y 2008 *Phys. Rev. Lett.* **100** 013601
- [7] Hartmann M J and Plenio M B 2008 *Phys. Rev. Lett.* **101** 200503
- [8] Borkje K, Nunnenkamp A and Girvin S M 2011 *Phys. Rev. Lett.* **107** 123601
- [9] König R, Maurer U and Renner R 2005 *IEEE Trans. Inform. Theory* **51** 2391
- [10] Bertrand J and Bertrand P 1987 *Found. Phys.* **17** 397–405
- [11] Vogel K and Risken H 1989 *Phys. Rev. A* **40** 2847–9
- [12] Smithey D T, Beck M, Raymer M G and Faridani A 1993 *Phys. Rev. Lett.* **70** 1244–7
- [13] Verlot P, Tavernarakis A, Briant T, Cohadon P-F and Heidmann A 2009 *Phys. Rev. Lett.* **102** 103601
- [14] Gröblacher S, Hammerer K, Vanner M R and Aspelmeyer M 2009 *Nature* **460** 724–7
- [15] Zwickl B M, Shanks W E, Jayich A M, Yang C, Bleszynski Jayich A C, Thompson J D and Harris J G E 2008 *Appl. Phys. Lett.* **92** 103125
- [16] Friedrich D, Kaufer H, Westphal T, Yamamoto K, Sawadsky A, Khalili F Y, Danilishin S, Goßler S, Danzmann K and Schnabel R 2011 *New J. Phys.* **13** 93017
- [17] Yamamoto K, Friedrich D, Westphal T, Goßler S, Danzmann K, Somiya K, Danilishin S L and Schnabel R 2010 *Phys. Rev. A* **81** 33849
- [18] Westphal T, Friedrich D, Kaufer H, Yamamoto K, Goßler S, Müller-Ebhardt H, Danilishin S L, Khalili Ya F, Danzmann K and Schnabel R 2012 *Phys. Rev. A* **85** 063806
- [19] Xuereb A, Schnabel R and Hammerer K 2011 *Phys. Rev. Lett.* **107** 213604
- [20] Jayich A M, Sankey J C, Zwickl B M, Yang C, Thompson J D, Girvin S M, Clerk A A, Marquardt F and Harris J G E 2008 *New J. Phys.* **10** 95008
- [21] Xiao M, Wu L-A and Kimble H J 1987 *Phys. Rev. Lett.* **59** 278–81
- [22] Grangier P, Slusher R E, Yurke B and LaPorta A 1987 *Phys. Rev. Lett.* **59** 2153–6
- [23] McKenzie K, Shaddock D A and McClelland D E 2002 *Phys. Rev. Lett.* **88** 231102
- [24] Eberle T, Steinlechner S, Bauchrowitz J, Händchen V, Vahlbruch H, Mehmet M, Müller-Ebhardt H and Schnabel R 2010 *Phys. Rev. Lett.* **104** 251102
- [25] The Ligo Scientific Collaboration 2011 *Nature Phys.* **7** 962–5